Journal of Engineering Science and Technology
Vol. 15, No. 4 (2020) 2163 - 2177

ESTIMATION OF SEDIMENTS TRANSPORT OF EUPHRATES RIVER BRANCHES WITHIN BABYLON CITY USING A MATHEMATICAL MODEL

NISREEN JASIM

Department of Environment Engineering,
University of Babylon, Hilla, 51002, Babylon, Iraq
E-mail: nassrin20052001@yahoo.com

Abstract

In this research, the estimation of sediment amount transported have been studied in six irrigation channels branched from Euphrates River. Six empirical methods for calculating the sediments capacity have been applied to these channels; namely Einstein-Brown, Blench, Inglis- Lasey, Laursen, Engelurd–Hansen, and Yang. Six monitoring stations along each channel were randomly selected to measure the hydraulic parameters, slope of the channel, and to collect sediments samples. Additionally, an empirical equation has been developed to calculate the sediment capacity in these irrigation channels depending on the collected data from the monitoring stations. The developed formula has been used to quantify the sediment load (concentration) in the reach of the river. The validity of this equation has been done by applying it to sets of experimental data collected from the monitoring stations. The predicted measurements, using this formula, were highly agreed with the experimental measurement (R^2 of 0.9972); therefore, the predicted formula gives less error, in comparison with the traditional formulas. This difference between the developed equation and the standard ones could be attributed to the limitations and assumptions used in the standard formulas. However, the Engelund Hansen, Blench, and Yang equations also showed good agreement with the measured field sediment discharge for almost of the studied channels with error percentages of 12.8% at Al-Mahaweel canal, 11.7% at Al-Hussayniya canal, and 13.6% at Bani-Hassan. The predicted formula gave the highest approximation to the sediment load at Euphrates River and Shatt Al-Hillah canal with error of 2.16% and 4.4%, respectively.

Keywords: Discharge, Irrigation channel, River, Sediment, Transport.

1. Introduction

Sediment transport is the movement of solid particles (sediment), typically due to a combination of gravity acting on the sediment, and/or the movement of the fluid in which the sediment is entrained. Sediment transport occurs in natural systems where the particles are clastic rocks (sand, gravel, boulders, etc.), mud, or clay; the fluid is air, water, or ice; and the force of gravity acts to move the particles along the sloping surface on which they are resting. Sediments transported by river and channel, they have direct or indirect influence on many of the commonly encountered problems such as improvement or stabilization of rivers or channels, flood ways for navigation, and flood control [1]. In addition, polluted sediments could cause serious water pollution phenomenon [2-6] that limits the availability of fresh water [7-10], which in turn requires the application of expensive water treatment methods [11-15], such as the electrochemical treatment [16-22], and biological units [23, 24]. Moreover, dredging of polluted sediments requires special solid management arrangements as it causes soil or ground water pollution [25]. Although some studies have been carried out to recycle dredged sediments and other types of solid wastes [26-30], handling of solid wastes is still very costly process [31-33]. Therefore, the presence of transportable sediments influences the planning and design of irrigation and drainage channels, sensitive turbines in hydro-electric power stations, and water facilities.

Measurement and estimation of bed load transport in different rivers are highly affected by its temporal fluctuations. Although, the temporal fluctuations are primarily driven by the flow regime, they are also associated with a variety of inherent channel processes, such as flow turbulence, grain entrainment, and bed forms migration. These internal and external controls often act at comparable time scales, and therefore difficult to disentangle, thus hindering the study of bed load variability under unsteady flow regime [34].

Analysis of velocity profiles plotted in defect form indicates that the Karman coefficient is independent of the amount of suspended sediment in an open channel flow. Contrary findings, based on earlier data by other workers, are due to error induced by ignoring the existence of the wake flow region. The wake strength coefficient is a function of the gross flow Richardson number [35]. With such a little incline, the channel can't move the whole load particularly when substantial dregs enter the waterway framework. Much of the time, some portion of the heap will be stored in the trench itself [36].

Reasons for sedimentation may incorporate regular events, changes in slope, disintegration and deterrent of trenches. In any case, a careful research work is required to confirm the genuine reasons for sedimentation. Along these lines, various investigations for managing silt in water system waterways have been completed around the world. For instance, an approach has been developed dependent on numerical displaying and effectively connected it on an optional system in Pakistan while proposing enhancements in the structure and desilting forms as an apparatus for longer conservation of value.

SETRIC (Sediment Transport in Irrigation Canals) model was applied to re-enact residue transport in water system plot in Nepal, while a numerical model was built and connected it to recreate silt in water system channels and discovered that it anticipated well the non-uniform dregs development in water system waterways.

It was discovered that it is conceivable to decrease dregs statement issue by appropriate plan and the board of the framework. An improvement was recommended in the waterway activity in an investigation of a water system plot in Pakistan. The author discovered that silt stores during low yield water prerequisite periods could be re-entrained during pinnacle water necessity periods. The effectiveness of the improved activity and upkeep on durable residue transport in Sudan were studied and discovered that the nonattendance of legitimate support exercises and water the board have a conspicuous job in expanding the affidavit along the water system waterways. Such examinations have not been completed in Mozambique. The majority of these examinations managed non-durable residue, with the exception of [37] which thought about strong silt. Furthermore, none of the studies brought out bits of knowledge on settling speeds at various profundities for a given channel reach.

The aim of the present research suggested an equation to calculate sediment capacity in these irrigation channels depending on the collected data and compare it with the experimental data and other empirical formulas for computing sediment capacity.

2. Studied area

Branches of Euphrates River are considered as one of the most important irrigation canals in the region because of the large areas that benefited from these branches. Therefore, the sediment transport in these branches has been studied by installing six monitoring stations along each one of these branches, as shown in Fig. 1.

Fig. 1. Case study of branches of Euphrates river.

The studied area was along the irrigation canals that take water from the Euphrates River directly in front of Hindyia barrage, with several channels that take water directly from the Shatt al-Hilla canal. The names and locations of the studied channels are:

I. The reach of Euphrates river after Hindyia barrage (its length within the boundaries of the province of Babylon is 121 km, and the average width is 71 m.
II. Al-Mahaweel canal: 20.6 km long and 7 m wide.
III. Shatt al-Hillah canal: its length within the boundaries of the province of Babylon is 101 km, and the average width is 77 m.
IV. Al-Mussayeb canal: with a length of 49.5 km and the width of 20.2 m.
V. Al-Hussayniya canal: 25 km in length and average width of 19 m.
VI. Bani-Hassan canal: 12 km long and average width of 14.4 m.

3. Theoretical Background

Sedimentation is the procedure by which diverse measured particles are shipped and saved into the water bodies and some other focuses along the water flow ways [38]. This work describes the role of sediment transport in the operation and maintenance of demand-based downstream controlled irrigation canals. Sediment deposition in these irrigation canals severely affects the operation of the automatic flow control system [39]. Contingent on the hydrodynamic conditions and residue attributes particles may move in three distinct structures, for example, bed burden, suspension and saltation forms [37].

Employing bed load formulae in hydraulic geometry relations were derived for stream width meander wavelength, and bed slope. The relations are in terms of friction factor, bed load discharge, bed load diameter, and water discharge. The bed load formulae are those of Shields (1936), Meyer-Peter and Muller (1948), Einstein (1950), and Engelund and Hansen (1966) [40].

Yilmaz [40] concluded that, Engelund and Hansen's condition ought to be connected to streams with rise beds as per the likeness guideline. As per Yang (1987), a stream can alter its harshness, geometry, profile and example through the procedures of dregs transport. Geologists and geomorphologists have made many of the subjective depictions of these dynamic changes of regular streams. Experimental system kinds of condition have been created by specialists to take care of plan issues. Endeavours have been made as of late to clarify these changes dependent on various extremal speculations and theories. Table 1 shows the formulas that mention above, and their parameters included.

Table 1. Formulas of computing sediment capacity with its parameters [41, 42].

Formula Name	Description parameters
Einstein-Brown (E-B) (1950)	$\emptyset = \frac{g_s}{\gamma_s F_1 \sqrt{g\,(\frac{\gamma_s}{\gamma-1}) d_s^3}}$ where: g_s: bed load sediment transport rate, γ, γ_s: specific weight of water and sediment, respectively, d_s: *sediment diameter,* F_1: the fraction of size class in the transported material ,φ = dimensionless bed load transport rate ; v : mean flow velocity ,according to above F_1 can be written as:

	$F_1 = \sqrt{\frac{3}{2} + \frac{36v^2}{gd_s^3(\frac{\gamma_s}{\gamma - 1})}} - \sqrt{\frac{36v^2}{gd_3(\frac{\gamma_s}{\gamma - 1})}}$
Laursen (L) (1958)	$X_{st} = 0.01\sum_1^p p\left(\frac{Dp}{d}\right)^{\frac{7}{6}}.\left(\frac{\tau o}{\tau c} - 1\right).f(\frac{V*}{wp})$ Where *Xst*: sediment concentration by weight per unit volume; *p*:fraction of the path size class of available sediment material; *N*: total number of size classes; *τc*: tractive and critical shear stress for the incipient motion of sediment size Dp, given by shields diagram; *τo*: bed shear stress due to grain roughness ;the function *f(v*/wp)* is given as two different curves for bed load and bed –material load ,therefore , Laursen formula can be used to determined either bed load or bed – material load.
Blench (B) (1964)	$V^2/g.d.So = (3.63/k).(1 + 105.x/233)(vb/ύ)1/4$ where: *K*: meander slope correction, *d*: mean depth, *b*: mean beneath; *V*: mean flow velocity; *g*: acceleration due to gravity; *So*: longitudinal slope of channel; *x* : specified distance ; *b*: width channel; *υ*: kinematic viscosity.
Engelund-Hansen's (E-H) (1966)	$g_s = 0.05\gamma_s V^2\sqrt{D_{50}/[g(\gamma_s/\gamma)]}\,[\tau_0/(\gamma_s - \gamma)D_{50}]^{3/2}$ where: g_s: sediment transports(weight) , ɤ, ɤs: specific weight of water and sediment ,respectively, *V*: mean flow velocity, D_{50}:sediment diameter, τ_o: bed shear stress.
Inglis-Lacey (I-L) (1977)	$g_s = 0.562\frac{vg^{1/3}}{W}\frac{V^2}{gd_{50}}\frac{\gamma V^3}{g}$ where *W*: sediment velocity for d_{50}, *gs*: sediment transports(weight); *V*: mean flow velocity; g: acceleration due to gravity; d_{50}: medium size of soil grain ; *υ*: kinematic viscosity.
Yange (Y) (1987)	$logC_l = 5.435 - 0.286\log\left(\omega\,{}^{D_{50}}/_{u}\right) - 0.457\log({}^{u_s}/_{\omega}) + [1.799 - 0.409\,log\left(\omega\,{}^{D_{50}}/_{u}\right) - 0.314\,log({}^{u_s}/_{\omega})]\log(V\,{}^{S}/_{\omega} - V_{cr}\,{}^{S}/_{\omega})$ Where: C_t: total average sediment concentrations in mg/l; *V*: mean flow velocity; u_*: shear velocity; V_{cr}: critical velocity; *S*: water surface slope; *ω*: fall velocity of sediment; D_{50}: sediment diameter; *υ*: kinematic viscosity.

4. Material and Methods

4.1. Sampling process and analyses

The fieldwork has been carried out, at six sections along the river and main channels, at different widths and depths as shown in Table 2. Value current meter was used to measure the velocities in these stations at depth 1.8 m; and consequently, the discharges in the stations were calculated. Six samples from the

bed materials were taken from each station, during the summer season, to evaluate the quality of the sediments. Sampling devices are shown in Fig. 2.

The sampling process started by lowering the sampler to the channel and keeping the nozzle closed by shutting the tube outlet. When the sampler reached the desire depth (3-5) m, the nozzle opened, hence, the air inside the bottle began to escape by the plastic tube and the water entered the bottle from the other opening to fill the bottle; then the sample dragged out of the channel [42, 43].

Table 2. Summary of hydraulic data.

Canal name	Width (B) (m)	Side slope (Z)	Longitudinal slope (S)	Flow rate (Q) (m^3/s)	Depth of canal (D) (m)
Euphrates river	72	9.0	1×10^{-4}	545	4.3
Al-Mahaweel canal	7	1.5	7.5×10^{-5}	12	1.5
Shatt Al-Hillah Canal	77	1.5	7.5×10^{-5}	250	3.2
Al-Mussayeb Canal	21	1.0	8.1×10^{-5}	70	3.5
Al-Hussayniya Canal	19	1.6	8×10^{-5}	10	1.7
Bani-Hassan canal	14.5	2.0	7.5×10^{-5}	5	1.3

(a) Preparation of sampling device for withdrawing sample of water.

(b) The steal holder and container for collection of composite water samples.

Fig. 2. Sampling devices.

Additionally, measurements included the relative density, and a volumetric analysis for the six samples at each section evenly distributed along the section and field discharge of sediments, as shown in Table 2. The distances and coordinates of all stations are listed in Table 3.

Volumetric distribution of channel soils represented by D_{50}, D_{65}, D_{35} were calculated from volumetric distribution curves, Table 4.

Table 3. Sections with the distances and coordinates [42].

Canal name	Distance	Location	Coordinates	
Euphrates river	0.00	950m Upstream of Al-hindyia barrage	447344E	3594258N
Al-Mahaweel canal	1.500	1500m D/S of Al-hindyia barrage	447553E	3591100N
Shatt Al-Hillah Canal	3.000	1500m D/S of Al-hindyia barrage	447472E	3591619N
Al-Mussayeb Canal	0.780	780m D/S of Al-hindyia barrage	447386E	3592376N
Al-Hussayniya Canal	2.730	2730m D/S of Al-hindyia barrage	447424E	3592114N
Bani-Hassan canal	2.240	1240m D/S of Al-hindyia barrage	447334E	3592595N

Table 4. Summary of sediment specification data.

Canal name	Relative density (γs) (gm/cm^3)	D_{50} (m)	D_{65} (m)	D_{35} (m)
Euphrates river	2.66	$15*10^{-6}$	$1*10^{-4}$	$54*10^{-5}$
Al-Mahaweel canal	2.7	$8*10^{-6}$	$7.5*10^{-5}$	$12*10^{-6}$
Shatt Al-Hillah Canal	2.69	$1.1*10^{-5}$	$7.5*10^{-5}$	$25*10^{-6}$
Al-Mussayeb Canal	2.7	$1.0*10^{-4}$	$8.1*10^{-5}$	$70*10^{-6}$
Al-Hussayniya Canal	2.72	$1.6*10^{-5}$	$8*10^{-5}$	$10*10^{-6}$
Bani-Hassan canal	2.68	$2.0*10^{-5}$	$7.5*10^{-5}$	$5*10^{-5}$

4.2. Experimental analysis of sediment

Filtration is one of the techniques used to break down the suspended strong focus. It includes the expulsion of the strong issue from an example by passing a known volume of the fluid strong blend through an appropriate channel. After fruition of filtration, the channel paper was dried and re gauged. The distinction between two weights isolated by the volume of the sample gives the centralization of the suspended dregs [43], as shown in Eq. (1)

$$C = \frac{(W_2 - W_1)}{V} \quad (1)$$

where: C = concentration of suspended sediment, mg/L.

w_1= weight of dry filter paper, mg.

w_2= weight of dry filter paper and suspended sediment, mg.

v = volume of sample.

Field Sediment Discharge explain in Table 5.

Table 5. Field sediment discharge.

Canal name	Concentration mg/L	Water flow rate m^3/s	Sediment flow rate kg/s
Euphrates river	72	9.0	$1*10^{-4}$
Al-Mahaweel canal	7	1.5	$7.5*10^{-5}$
Shatt Al-Hillah Canal	77	1.5	$7.5*10^{-5}$
Al-Mussayeb Canal	21	1.0	$8.1*10^{-5}$
Al-Hussayniya Canal	19	1.6	$8*10^{-5}$
Bani-Hassan canal	14.5	2.0	$7.5*10^{-5}$

5. Results and Discussion

5.1. Dimensional Analysis of Sediment Variables

An empirical formula has been developed in the current study to quantify the sediment load (concentration) in the studied irrigation channels. This formula obtained depending on data collected from six different cross-sections.

The variables utilized for field and lab work and their relationship can be given as follow:

$$F1(\rho s, \rho w, D35, D65, V, Rh, S, g, Qs) = 0 \quad (2)$$

By dimensional analysis, this equation can be written as:

$$Qs/(\rho s.g^{0.5}.D_{35}^{2.5}) = F_2(\frac{Rh}{D_{35}}, g.\frac{D_{35}}{V_2}, S, \frac{D_{35}}{D_{65}}, \rho s/\rho w) = 0 \quad (3)$$

The sediment discharge given in the following Eq. (4) resulted from a regression analysis by MS-statistical:

$$Qs = ((R_h.\frac{S_g-1}{V}) + (\frac{D_{35}.D_{65}}{2S})^{-0.56})^{1.2} \quad (4)$$

where, Q_s= total sediment load (kg/s); V= mean velocity of flow (m/s); g= gravitational acceleration (m/sec^2); R_h= hydraulic radius (m); S_g= specific gravity; S= slope of the channel; D_{35}, D_{65}= particle size for which 35% and 65% by weight of sediment is finer (mm).

The coefficient of variance for Eq. (4) was found to be equal to 0.87. It is noteworthy to highlight that the variables that used in the development of Eq. (4) have been selected according to the relevant literature [1]. Equation (4) was found to fit every one of the studied channels as the correlation coefficient between the predicted values (of this equation) and the measured values is R^2=0.9972, as shown in Fig. 3.

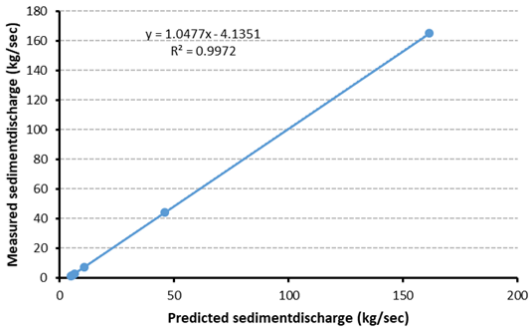

Fig. 3. Comparison between observed and predicted values of sediment discharges for the studied cross-sections.

5.2. Comparison with the formulas

The most widely used engineering and mathematical methods for calculation of sediment separation are Einstein-Brown (E-B), Blench (B), Inglis- Lasey (I-L), Laursen (L), Engelurd–Hansen (E-H), and Yang (Y) equations.

After the application of mathematical methods to the collected data from the studied channels, the sediment capacity was calculated by applying the suggested formula to the same data, Table 6.

The soil of riverbed at these locations can be considered as the reason for the differences in sediment discharge, where it has been noticed that soil type in the large canals was rough and homogeneous. While, in small canals, the soil was smooth and relatively nonhomogeneous. In terms of the geometry of the canals, it has been noticed that the cross-section of the studied canals was generally a rounded or a trapezoidal section.

Table 6. Predicted values of sediment capacity discharge (in kg/s).

Canal name	E-B	B	I-L	La	E-H	Y	Developed formula	Field sediment discharge
Euphrates river	56	22.3	7129	32.6	4.76	54.3	161.43	165
Al-Mahaweel canal	0.64	16.1	63.8	92.4	2.18	1.17	6.32	2.5
Shatt Al-Hillah Canal	19.5	34.8	4320	84.1	0.12	8.46	45.94	44
Al-Mussayeb Canal	4.7	20.9	65.2	54.3	4.67	8.88	10.72	7.1
Al-Hussayniya Canal	0.45	1.9	2.67	2.9	6.69	26.3	5.56	1.7
Bani-Hassan canal	0.12	2.1	7.32	7.5	7.79	0.95	4.99	1.1

According to the obtained results, the predicted sediment discharge by the developed formula is in a good agreement with field measurement at Euphrates River, Shatt Al-Hillah canal, and Al-Mussayeb canal, but not agreed with those at the rest of the channels.

Additionally, it has been found the Engelurd–Hansen (E-H) is in a good agreement with the field measurements at Al-Mahaweel canal, Blench (B) agreed with the field measurements at Al-Hussayniya canal, and Yang (Y) yields close results to the field measurements at Al-Mussayeb canal.

The difference in measured and predicted sediment discharge (between the developed formula and the standard formulas) could be attributed to the limitations and assumptions used in standard formulas.

It was also found that each one of the standard formulas gave results of sediments flow rate different from the other under the same discharge and hydraulics conditions. To find out which one of the used formula was the best to predict the sediment discharge in the entire channel, a percentage of error was

applied to the results of developed and standard formulas; percentage of error is calculated using the following formula [44]:

$$Error\% = \frac{(X_1 - X_2)}{X_1} \times 100 \quad (5)$$

where, in this study, X_1 and X_2 represent the measured and predicted sediment, respectively.

The calculated percentages of error are in Table 7.

Table 7. Percentages error of sediment discharge for different channels.

Canal name	E-B error %	B error %	I-L error %	L error %	E-H error %	Y error %	Suggested Formula error%
Euphrates river	66	86.4	-4220	80.2	97.1	67.08	2.16
Al-Mahaweel Canal	74.4	-544	-2452	-3596	12.8	53.2	60.44
Shatt Al-Hillah Canal	55.6	20.9	-9718	-91.1	99.7	80.7	4.40
Al-Mussayeb Canal	33.8	-194.3	-818.3	-664.7	34.2	-25	50.98
Al-Hussayniya Canal	73.5	-11.7	-57.05	-70.5	-293.5	-1445	227
Bani-Hassan Canal	89	-90.9	-565.4	-581.8	-608.1	13.6	353

According to Table 7, for Euphrates River, the most suitable formula that achieved minimum percentage of error were Einstein-Brown and Yange, with values, respectively. While in Al-Mahaweel canal, the best results were obtained from Engelund Hansen formula. It should be noted that these formulas are based mostly on flume studies that employed uniformly sized and shaped sediment.

For Shatt al-Hillah canal, the most suitable formula that achieved the minimum percentage of error was Blench formula. While in Al-Mussayeb canal, the best results were obtained by applying Einstein-Brown and Engelund Hansen formulas. This could be attributed to the fact that these formulas depend generally on flume, properties about that utilized consistently measured and formed silt.

For Al-Hussayniya canal, the most suitable formula that achieved minimum percentage of error was Blench. While in Bani-Hassan canal, the best results were obtained by applying Yange formula.

It can be concluded from the results above that the developed formula gives less error in comparison with the standard formulas. Additionally, it can be noticed that the developed formula gave the highest approximation to the sediment load at Euphrates River and Shatt Al-Hillah canal with percentage of error of 2.16% and 4.4%, respectively.

Among the six equations that used in this study, the Engelund Hansen, Blench and Yang equations showed good agreement with the measured field sediment discharge for most of the studied canals with percentages of error of 12.8% at Al-Mahaweel canal, 11.7% at Al-Hussayniya canal, and 13.6% at Bani-Hassan canal, respectively. Finally, sensing technology has been used in different monitoring and

controlling processes [45-48]; therefore this technology could be used, in future researches, to monitor the transportation of sediments.

6. Conclusions

Main conclusions of the present investigation are as follows:

- The outcomes of this study indicated the calculation of sediments, under the same hydraulic conditions, were varied due to the limitations and assumptions used in standard formulas, thus, it cannot be adopted in the studied case.
- High agreement was noticed between the field measurement of sediment discharge and the estimated the sediment discharge by Engelund Hansen, Blench, and Yang equations. This result confirms the applicability of the mentioned equations to estimate the sediment discharge in Al-Mahaweel canal, Al-Hussayniya canal, and Bani-Hassan canal.
- According to the measured and predicated sediment load, the developed formula is applicable to estimate the sediment load at Euphrates River and Shatt Al-Hillah canal as the error percent was very low (error of 2.16 and 4.4% for Euphrates River and Shatt Al-Hillah canal, respectively).

Nomenclatures

B	Width of canal, m
C	Concentration of suspended sediment, mg/L
D	Depth canal, m
D_{35}, D_{65}	Particle size for which 35% and 65% by weight of sediment is finer, mm
D_{50}	Particle size for which 50% by weight of sediment is finer, mm
g	Gravitational acceleration, m/s^2
Q	Flow rate, m^3/s
Q_s	Total sediment load, kg/s
R_h	Hydraulic radius
S	Slope of the channel, m
S_g	Specific gravity
v	Volume of sample, m^3
w_1	Weight of dry filter paper, mg (mg)
w_2	Weight of dry filter paper and suspended sediment, m (mg)
Z	Side slope

Greek Symbols

γs	Relative density, kg/m^3

References

1. Al-Kizwini, M.J.; Khassaf, S.I.; and Bahjat, A.N. (2007). Evaluation of Sediment transport in Kirkuk irrigation channel. *Engineering and Technology Journal*, 25(3), 349-357.
2. Al-Saati, N.H.; Hussein, T.K.; Abbas, M.H.; Hashim, K.; Al-Saati, Z.N.; Kot, P.; Sadique, M.; Aljefery, M.H.; and Carnacina, I. (2019). Statistical modelling

of turbidity removal applied to non-toxic natural coagulants in water treatment: a case study. *Desalination and Water Treatment*, 150, 406-412.

3. Omran, I.I.; Al-Saati, N.H.; Hashim, K.S.; Al-Saati, Z.N.; P., K.; Khaddar, R. A.; Al-Jumeily, D.; Shaw, A.; Ruddock, F.; and Aljefery, M. (2019). Assessment of heavy metal pollution in the Great Al-Mussaib irrigation channel. *Desalination and Water Treatment*, 168, 165-174.
4. Al-Jumeily, D.; Hashim, K.; Alkaddar, R.; Al-Tufaily, M.; and Lunn, J. (2018). Sustainable and Environmental Friendly Ancient Reed Houses (Inspired by the Past to Motivate the Future). *Proceedings of the 11th International Conference on Developments in eSystems Engineering (DeSE)*. Cambridge, UK, 214-219.
5. Zubaidi, S.L.; Al-Bugharbee, H.; Muhsen, Y.R.; Hashim, K.; Alkhaddar, R.M.; Al-Jumeily, D.; and Aljaaf, A.J. (2019). The Prediction of Municipal Water Demand in Iraq: A Case Study of Baghdad Governorate. *Proceedings of the 12th International Conference on Developments in eSystems Engineering (DeSE)*. Kazan, Russia, 274-277.
6. Zubaidi, S.; Al-Bugharbee, H.; Ortega Martorell, S.; Gharghan, S.; Olier, I.; Hashim, K.; Al-Bdairi, N.; and Kot, P. (2020). A Novel Methodology for Prediction Urban Water Demand by Wavelet Denoising and Adaptive Neuro-Fuzzy Inference System Approach. *Water*, 12(6), 1-17.
7. Hashim, K.S. (2017). *The innovative use of electrocoagulation-microwave techniques for the removal of pollutants from water*. Ph.D. Thesis. Civil Engineering Liverpool John Moores University, Liverpool, United Kingdom.
8. Zubaidi, S.L.; Kot, P.; Hashim, K.; Alkhaddar, R.; Abdellatif, M.; and Muhsin, Y.R. (2019). Using LARS –WG model for prediction of temperature in Columbia City, USA. *Proceedings of the First International Conference on Civil and Environmental Engineering Technologies (ICCEET)*. University of Kufa, Iraq, 31-38.
9. Zubaidi, S.L.; Ortega-Martorell, S.; Al-Bugharbee, H.; Olier, I.; Hashim, K.S.; Gharghan, S.K.; Kot, P.; and Al-Khaddar, R. (2020). Urban Water Demand Prediction for a City that Suffers from Climate Change and Population Growth: Gauteng Province case study. *Water*, 12(7), 1-18.
10. Zubaidi, S.L.; Ortega-Martorell, S.; Kot, P.; Alkhaddar, R.M.; Abdellatif, M.; Gharghan, S.K.; Ahmed, M.S.; and Hashim, K. (2020). A Method for Predicting Long-Term Municipal Water Demands Under Climate Change. *Water Resources Management*, 34(3), 1265-1279.
11. Hashim, K.S.; Alkhaddar, R.; Shaw, A.; Kot, P.; Al-Jumeily, D.; Alwash, R.; and Aljefery, M.H. (2020). *Electrocoagulation as an eco-friendly River water treatment method, in Advances in Water Resources Engineering and Management* (1st ed.). Berlin: Springer.
12. Hashim, K.S.; Shaw, A.; Al Khaddar, R.; Ortoneda Pedrola, M.; and Phipps, D. (2017). Defluoridation of drinking water using a new flow column-electrocoagulation reactor (FCER) - Experimental, statistical, and economic approach. *Journal of Environmental Management*, 197, 80-88.
13. Hashim, K.S.; Shaw, A.; Al Khaddar, R.; Pedrola, M.O.; and Phipps, D. (2017). Iron removal, energy consumption and operating cost of electrocoagulation of drinking water using a new flow column reactor. *Journal of Environmental Management*, 189, 98-108.

14. Hashim, K.S.; Shaw, A.; Al Khaddar, R.; Pedrola, M.O.; and Phipps, D. (2017). Energy efficient electrocoagulation using a new flow column reactor to remove nitrate from drinking water - Experimental, statistical, and economic approach. *Journal of Environmental Management*, 196, 224-233.
15. Hashim, K.S.; Khaddar, R.A.; Jasim, N.; Shaw, A.; Phipps, D.; Kota, P.; Pedrola, M.O.; Alattabi, A.W.; Abdulredha, M.; and Alawsh, R. (2019). Electrocoagulation as a green technology for phosphate removal from River water. *Separation and Purification Technology*, 210, 135-144.
16. Hashim, K.S.; Al-Saati, N.H.; Alquzweeni, S.S.; Zubaidi, S.L.; Kot, P.; Kraidi, L.; Hussein, A.H.; Alkhaddar, R.; Shaw, A.; and Alwash, R. (2019). Decolourization of dye solutions by electrocoagulation: an investigation of the effect of operational parameters. *Proceedings of the First International Conference on Civil and Environmental Engineering Technologies (ICCEET)*. University of Kufa, Iraq, 25-32.
17. Abdulhadi, B.A.; Kot, P.; Hashim, K.S.; Shaw, A.; and Khaddar, R.A. (2019). Influence of current density and electrodes spacing on reactive red 120 dye removal from dyed water using electrocoagulation/electroflotation (EC/EF) process. *Proceedings of the First International Conference on Civil and Environmental Engineering Technologies (ICCEET)*. University of Kufa, Iraq, 12-22.
18. Emamjomeh, M.M.; Mousazadeh, M.; Mokhtari, N.; Jamali, H.A.; Makkiabadi, M.; Naghdali, Z.; Hashim, K.S.; and Ghanbari, R. (2019). Simultaneous removal of phenol and linear alkylbenzene sulfonate from automotive service station wastewater: Optimization of coupled electrochemical and physical processes. *Separation Science and Technology*, 1, 1-11.
19. Hashim, K.; Kot, P.; Zubaid, S.; Alwash, R.; Al Khaddar, R.; Shaw, A.; Al-Jumeily, D.; and Aljefery, M. (2020). Energy efficient electrocoagulation using baffle-plates electrodes for efficient Escherichia Coli removal from Wastewater. *Journal of Water Process Engineering*, 33(20), 1-7.
20. Hashim, K.S.; Hussein, A.H.; Zubaidi, S.L.; Kot, P.; Kraidi, L.; Alkhaddar, R.; Shaw, A.; and Alwash, R. (2019). Effect of initial pH value on the removal of reactive black dye from water by electrocoagulation (EC) method. *Proceedings of the 2nd International Scientific Conference*. Al-Qadisiyah University, Iraq 12-22.
21. Hashim, K.S.; Idowu, I.A.; Jasim, N.; Al Khaddar, R.; Shaw, A.; Phipps, D.; Kot, P.; Pedrola, M.O.; Alattabi, A.W.; and Abdulredha, M. (2018). Removal of phosphate from River water using a new baffle plates electrochemical reactor. *MethodsX*, 5, 1413-1418.
22. Hashim, K.S.; Ali, S.S. M.; Alrifaie, J.K.; Kot, P.; Shaw, A.; Khaddar, R.A.; Idowu, I.; and Gkantou, M. (2020). Escherichia coli inactivation using a hybrid ultrasonic–electrocoagulation reactor. *Chemosphere*, 247, 1-7.
23. Alattabi, A.W.; Harris, C.; Alkhaddar, R.; Alzeyadi, A.; and Hashim, K. (2017). Treatment of Residential complexes' wastewater using environmentally friendly technology. *Procedia Engineering*, 196, 792-799.
24. Alattabi, A.W.; Harris, C.B.; Alkhaddar, R.M.; Hashim, K.S.; Ortoneda-Pedrola, M.; and Phipps, D. (2017). Improving sludge settleability by introducing an innovative, two-stage settling sequencing batch reactor. *Journal of Water Process Engineering*, 20, 207-216.

25. Hashim, K.S.; Al-Saati, N.H.; Hussein, A.H.; and Al-Saati, Z.N. (2018). An investigation into the level of heavy metals leaching from canal-dreged sediment: a case study metals leaching from dreged sediment. *Proceedings of the First International Conference on Materials Engineering & Science*. Istanbul Aydın University (IAU), Turkey, 12-22.
26. Manap, N.; Polis, S.; Sandirasegaran, K.; Masrom, M.N.; Chen, G.K.; and Yahya, M.Y. (2016). Strength of concrete made from dredged sediments. *Jurnal Teknologi*, 78(3), 111-116.
27. Shubbar, A.A.; Jafer, H.; Dulaimi, A.; Hashim, K.; Atherton, W.; and Sadique, M. (2018). The development of a low carbon binder produced from the ternary blending of cement, ground granulated blast furnace slag and high calcium fly ash: An experimental and statistical approach. *Construction and Building Materials*, 187, 1051-1060.
28. Shubbar, A.A.; Al-Shaer, A.; Alkizwini, R.S.; Hashim, K.; Hawesah, H.A.; and Sadique, M. (2019). Investigating the influence of cement replacement by high volume of GGBS and PFA on the mechanical performance of cement mortar. *Proceedings of the First International Conference on Civil and Environmental Engineering Technologies (ICCEET)*. University of Kufa, Iraq, 31-38.
29. Shubbar, A.A.; Sadique, M.; Shanbara, H.K.; and Hashim, K. (2020). *The Development of a New Low Carbon Binder for Construction as an Alternative to Cement, in Advances in Sustainable Construction Materials and Geotechnical Engineering* (1st ed.). Berlin: Springer.
30. Majdi, H.S.; Shubbar, A.; Nasr, M.S.; Al-Khafaji, Z.S.; Jafer, H.; Abdulredha, M.; Al Masoodi, Z.; Sadique, M.; and Hashim, K. (2020). Experimental data on compressive strength and ultrasonic pulse velocity properties of sustainable mortar made with high content of GGBFS and CKD combinations. *Data in Brief*, 31, 1-11.
31. Abdulredha, M.; Al Khaddar, R.; Jordan, D.; Kot, P.; Abdulridha, A.; and Hashim, K. (2018). Estimating solid waste generation by hospitality industry during major festivals: A quantification model based on multiple regression. *Waste Management*, 77, 388-400.
32. Abdulredha, M.; Rafid, A.; Jordan, D.; and Hashim, K. (2017). The development of a waste management system in Kerbala during major pilgrimage events: determination of solid waste composition. *Procedia Engineering*, 196, 779-784.
33. Idowu, I.A.; Atherton, W.; Hashim, K.; Kot, P.; Alkhaddar, R.; Alo, B.I.; and Shaw, A. (2019). An analyses of the status of landfill classification systems in developing countries: Sub Saharan Africa landfill experiences. *Waste Management*, 87, 761-771.
34. Redolfi, M.; Bertoldi, W.; Tubino, M.; and Welber, M. (2018). Bed load variability and morphology of gravel bed rivers subject to unsteady flow: A laboratory investigation. *Water Resources Research*, 54(2), 842-862.
35. Coleman, N.L. (1981). Velocity profiles with suspended sediment. *Journal of Hydraulic Research*, 19(3), 211-229.
36. Cook, A.C. (2008). *Comparison of one-dimensional HEC-RAS with two-dimensional FESWMS model in flood inundation mapping*. M.Sc. Thesis, Graduate School, Purdue University, United States.

37. Osman, I.E. (2015). *Impact of improved operation and maintenance on cohesive sediment transport in Gezira Scheme, Sudan* (1st ed.). Delft: UNESCO-IHE Institute Press.
38. Kim, J.; Ivanov, V.Y.; and Katopodes, N.D. (2013). Modeling erosion and sedimentation coupled with hydrological and overland flow processes at the watershed scale. *Water Resources Research*, 49(9), 5134-5154.
39. Munir, S. (2011). *Role of Sediment Transport in Operation and Maintenance of Supply and Demand Based Irrigation Canals: Application to Machai Maira Branch Canals* (1st ed.). London: CRC Press.
40. Yilmaz, L. (2015). *General Hydraulic Geometry in: Effects of Sediment Transport on Hydraulic Structures* (1st ed.). Croatia: INTECH.
41. Hossain, M.M.; and Rahman, M.L. (1998). Sediment transport functions and their evaluation using data from large alluvial rivers of Bangladesh. *IAHS-AISH Publication*, 249, 375-382.
42. Wro, I. (2018). *Planning and follow-up section, manual for measuring hydraulic parameters*. *Water resources*, 43, 20-28.
43. Yadav, S.; and Samtani, B. (2010). Evaluation and Improvement of Bed Load Formula Using Tapi River Data, India. *Journal of Water Resource and Protection*, 2(03), 245-250.
44. Pallant, J. (2005). *SPSS survival manual* (2nd ed.). Sydney: McGraw-Hill Inc.
45. Gkantou, M.; Muradov, M.; Kamaris, G.S.; Hashim, K.; Atherton, W.; and Kot, P. (2019). Novel Electromagnetic Sensors Embedded in Reinforced Concrete Beams for Crack Detection. *Sensors*, 19(23), 5175-5189.
46. Ryecroft, S.; Shaw, A.; Fergus, P.; Kot, P.; Hashim, K.; Moody, A.; and Conway, L. (2019). A First Implementation of Underwater Communications in Raw Water Using the 433 MHz Frequency Combined with a Bowtie Antenna. *Sensors*, 19(8), 1813.
47. Ryecroft, S.P.; Shaw, A.; Fergus, P.; Kot, P.; Hashim, K.; and Conway, L. 2020). A Novel Gesomin Detection Method Based on Microwave Spectroscopy. *Proceedings of the 12th International Conference on Developments in eSystems Engineering (DeSE)*. Kazan, Russia, 14-23.
48. Teng, K.H.; Kot, P.; Muradov, M.; Shaw, A.; Hashim, K.; Gkantou, M.; and Al-Shamma'a, A. (2019). Embedded Smart Antenna for Non-Destructive Testing and Evaluation (NDT&E) of Moisture Content and Deterioration in Concrete. *Sensors*, 19(3), 547-559.